ON THE USE OF SHOCK TUNNELS FOR RESEARCH ON HYPERSONIC FLOW

By D. W. HOLDER and D. L. SCHULTZ

National Physical Laboratory, Teddington, Middlesex, England

Summary—The paper gives brief details of the shock tubes and shock tunnels that are in use at the N.P.L., and outlines recent research on the duration of uniform flow in shock tunnels operated by the reflected-shock technique. Particular attention is given to the effects of disturbances reflected from the contact surface, and of the expansion wave originating at the diaphragm. The results suggest that, over a useful range of shock Mach number, the pressure at the nozzle entry can be maintained reasonably constant for a period which is long compared with the time required to establish steady flow past the model under test, and which should permit many aerodynamic measurements to be made. Recent N.P.L. work on the development of suitable measuring techniques is summarized.

1. INTRODUCTION

A general review[1] of the facilities that may be used for laboratory studies of hypersonic flow was presented at the first meeting of the I.C.A.S. Particular attention was given to the "Hotshot" tunnel, and it was suggested that, although the shock tube could play an important part, the shock tunnel had severe limitations for aerodynamic testing, mainly because of its very short running time.

The value of the shock tube would be generally agreed, but the authors feel that the shock tunnel, also, has a useful place in hypersonic research. To illustrate this view, the present paper discusses recent work at the N.P.L. on the development of shock tunnels and associated instrumentation, and on investigations of the uniformity and duration of the test flow that they provide.

2. THE SHOCK TUBES AND SHOCK TUNNELS AT THE NATIONAL PHYSICAL LABORATORY

The leading dimensions and details of the shock tubes and shock tunnels that are at present in use at the N.P.L. are set out in Table 1. They are intended to supplement a helium tunnel, a low-density tunnel, and a tunnel using air heated to avoid liquefaction at Mach numbers up to 7 in providing a set of facilities for fundamental research on most aspects of hypersonic flow. A small "Hotshot" tunnel has also recently been built for research on its flow properties, and a magnetically-driven shock tube is being developed for research on magnetogasdynamics.

The shock tubes are driven by hydrogen at maximum pressures ranging from 130 to 1000 atmospheres, and, except for one tube the initial hydrogen temperature is atmospheric.

TABLE 1

Shock Tubes and Shock Tunnels at the National Physical Laboratory

Cross-section of tube	Overall length of tube	Maximum driving pressure	Cross-section of expanded working section
Inches	Feet	Atmospheres	Inches
6 dia.	57·5	1000	30 or 16 dia.
3 dia.	46·0	130	16 or 8 dia.
2 dia.	21·0	1000	8 dia.
6 by $3^1/_2$	18·0	500	—
2 dia.	14·0	130	—
2 dia.	21·0	130	—
2 dia.	13·0	400*	—

* The hydrogen may be heated electrically to 300°C.

No new principles are involved in the construction of these facilities, and it will suffice to give a brief description of one of them which is illustrated in Fig. 1. The driving tube is of 6 in. bore, and is stressed to withstand 1000 atmospheres. Two diaphragm stations are provided to enable the time of arrival of the expansion wave at the nozzle entry to be adjusted (see section 3.2.3.), or to enable the double-diaphragm driving technique[2] to be used for the production of fast shocks. An unexpanded working section is available for tests not requiring Mach number simulation, and the entry to the expansion nozzle can be readily changed so that the facility can operate either as a "straight-through" or reflected-shock tunnel. The nozzle is conical, and the area ratio is adjusted by altering either the entry or throat diameter, depending on whether "straight-through" or reflected-shock operation is used. The nozzle diaphragm is placed upstream of the entry or near the throat, and the nozzle, working section and dump tank can be evacuated to 5 μ of mercury to reduce the nozzle starting time.

3. THE FLOW PROVIDED BY A SHOCK TUNNEL

In many laboratories, considerable effort has been devoted to research aimed at assessing the duration and properties of the test flow provided by shock tunnels. The useful duration of flow depends on the duration at

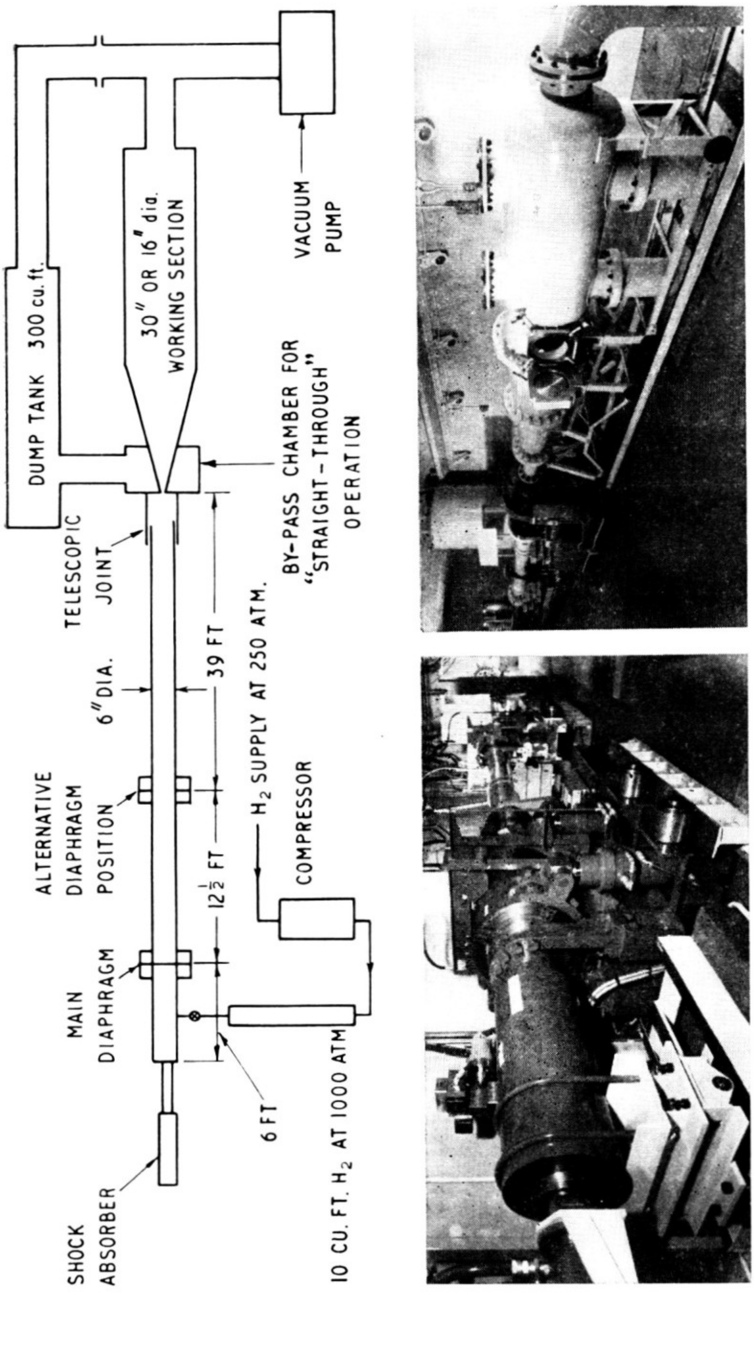

FIG. 1. N.P.L. 6 in. dia. shock tunnel. Arrangement for reflected-shock operation.

entry to the nozzle, and on the losses of testing time associated with the expansion process in the nozzle, and in the establishment of steady flow past the model under test. The properties of the test flow depend on such factors as the boundary-layer growth in the nozzle and, at high stagnation enthalpies, the extent to which recombination or deionization occur in equilibrium with the local temperatures when the flow is expanded[3, 4, 5].

The variation of the flow properties with time has formed the subject of several investigations at the N.P.L. Because "straight-through" operation has several advantages, early work was confined to shock tunnels of this type. Unfortunately, it was found[6] that the loss of testing time arising[7] from the presence of the expansion nozzle was often comparable to the duration of uniform flow at its entry, so that the useful testing time was extremely short. Recent work has, accordingly, concentrated on reflected-shock operation, and, after a brief discussion of the extent to which a shock tunnel of this type can simulate full-scale flight, typical results are reviewed below.

3.1. *Aerodynamic Simulation*

The extent to which various hypersonic test facilities can simulate full-scale values of the appropriate aerodynamic parameters has been considered by several authors (see, for example, refs. 1–8) and typical data for the largest N.P.L. shock tunnel only will be reproduced here. A conventional plot of Reynolds number per foot against flight velocity at various altitudes is given in Fig. 2. Values of the maximum Reynolds number attainable in the shock tunnel with correct Mach number and stagnation specific enthalpy simulation are superimposed for reflected-shock operation with a maximum pressure of 1000 atmospheres. It is seen that there is a rapid fall of Reynolds number working-section Mach numbers, M_w, greater than about 10. The advantages to be gained from even a small reduction in the test Mach number below the full-scale value are evident from the alternative curve which shows the simulation conditions if the Mach number M_w is held constant at 9·85. When, for example, the tube is operated at the stagnation temperature corresponding to flight at a Mach number of 11·2, a gain of 100 times in Reynolds number is achieved by reducing the test Mach number to 9·85. It is, thus, important to consider the relative importance of Mach and Reynolds number simulation in experiments at high Mach number.

3.2. *The Flow Duration in Reflected-Shock Tunnels*

For reflected-shock operation, the end of the tube is closed, as sketched in Fig. 3, apart from the small nozzle entry, and primary shock is reflected in order to bring the flow and contact surface approximately

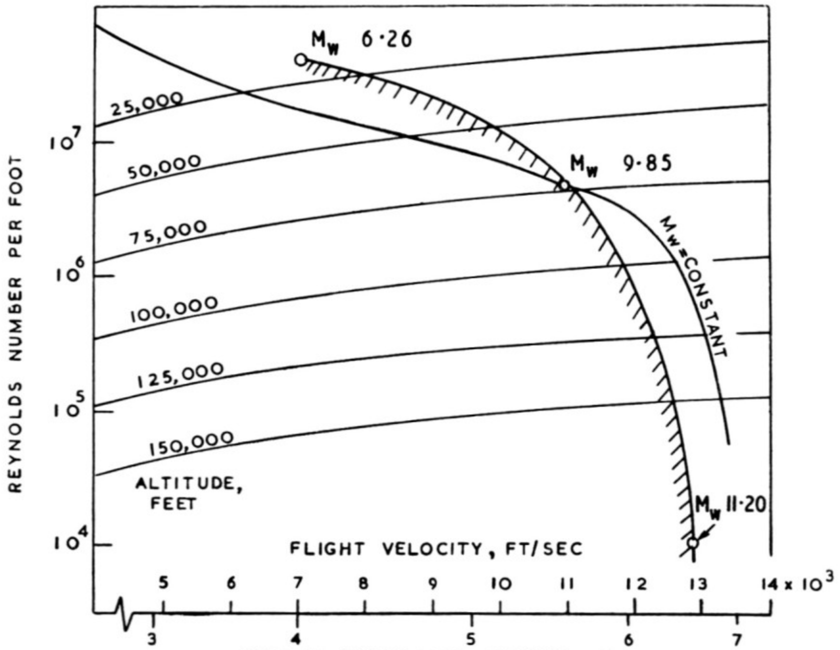

FIG. 2. Limit (shown hatched) for simulation of full-scale mach number, stagnation enthalpy, and Reynolds number per foot in the N.P.L. 6 in shock tunnel. H_2/air.

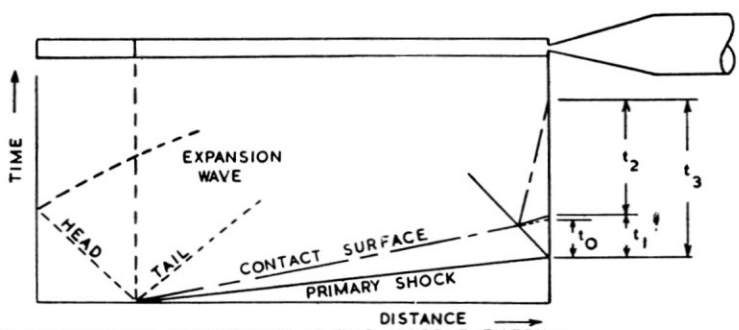

DURATION OF UNIFORM CONDITIONS AT THE NOZZLE ENTRY :-

t_0 STRAIGHT-THROUGH SHOCK TUNNEL, LIMITED BY ARRIVAL OF CONTACT SURFACE.

t_1 REFLECTED-SHOCK TUNNEL, LIMITED BY FIRST DISTURBANCE REFLECTED BY CONTACT SURFACE.

t_2 LIMITED BY ARRIVAL OF CONTACT SURFACE ASSUMING SUBSEQUENT REFLECTIONS WEAK.

t_3 LIMITED BY ARRIVAL OF CONTACT SURFACE ASSUMING NO REFLECTIONS ("TAILORED").

FIG. 3. Wave diagram for a reflected-shock tunnel.

to rest, apart from the small velocity associated with the flow the nozzle. Provided that the conditions behind the reflected shock remain sufficiently uniform, the whole of the shock-heated gas may then be used to supply the nozzle, in contrast to the "straight-through" shock tunnel where most of it is wasted in the by-pass system. The flow duration is, thereby, greatly increased (from t_0 to t_3).

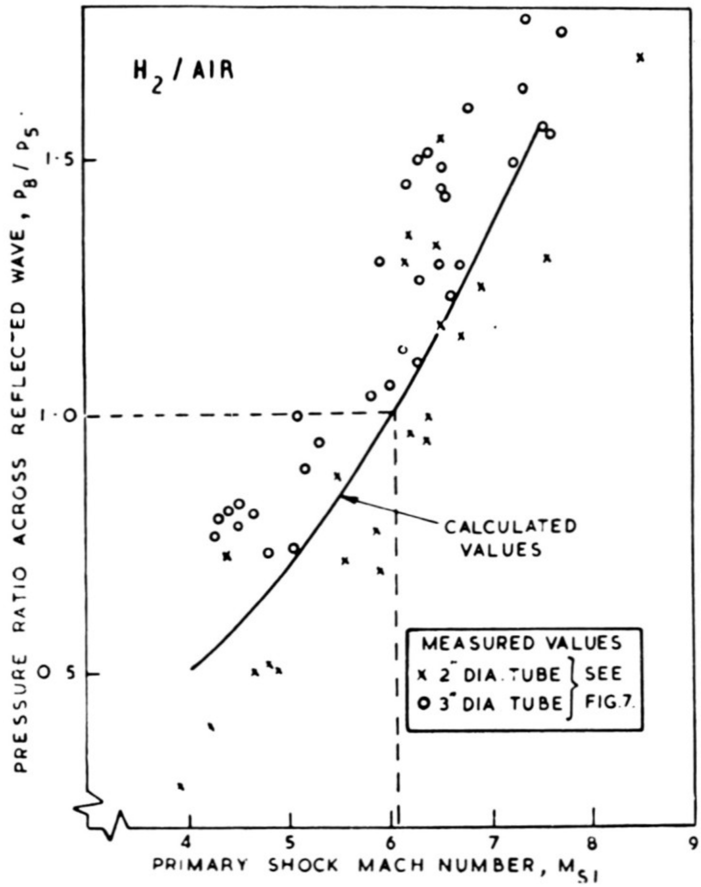

FIG. 4. Pressure ratio across the disturbance reflected from the contact surface (for notation see FIG. 6).

The uniformity may be affected by disturbances reflected from the contact surface, or by the arrival of the expansion wave originating at the primary diaphragm.

3.2.1. *Disturbances reflected from the contact surface*—When the shock, reflected from the effectively closed end of the tube, strikes the contact surface, there will be a transmitted shock and a reflected disturbance which may be either a shock or an expansion wave. Since the reflected disturbance will eventually reach the nozzle entry, it is important to understand the factors influencing its strength. Values computed[9] by perfect-gas theory are shown in Fig. 4 for hydrogen driving air, both at initially atmo-

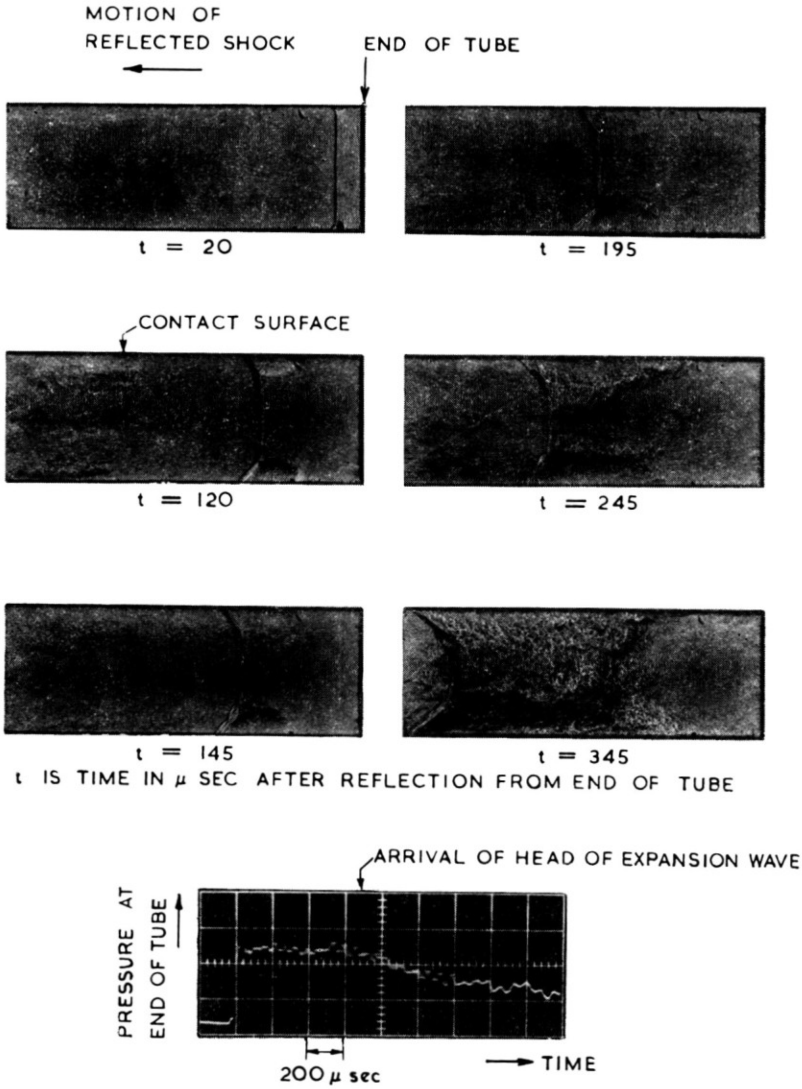

FIG. 5. Photographs of the interaction of the reflected shock with the boundary layer and contact surface. H_2/air, $M_{s1} = 6$.

spheric temperature. It is seen that for one value of the primary shock Mach number the reflected disturbance is a Mach wave (i.e. the pressure ratio is unity). The potential importance of this condition in shock-tube operation was first suggested by Wittliff *et al.*[10], who referred to a contact surface arranged to produce no wave reflection as "tailored". Schlieren photographs taken[11] in a tube of 6 in. by $3\frac{1}{2}$ in. cross section, and illustrating the motion of the reflected shock, and its interaction with the boundary layer and the contact surface, are reproduced in Fig. 5. As predicted by simple theory, the contact surface is brought effectively to rest, and no reflected disturbance can be detected. A pressure record measured near the reflecting wall shows that the pressure remains substantially constant until the arrival of head of the expansion wave originating at the diaphragm.

It appears from Fig. 4 that the pressure change associated with the disturbance reflected from the contact surface can be accepted only at Mach numbers very close to the "tailored" value (e.g. $5{\cdot}7 < M_{s1} < 6{\cdot}3$ if the pressure is to be constant to ± 10 per cent with unheated hydrogen driving air). It is also clear, that if the flow duration (t_1 in Fig. 3) is limited by the arrival of the reflected disturbance, it will be little greater than for "straight-through" operation.

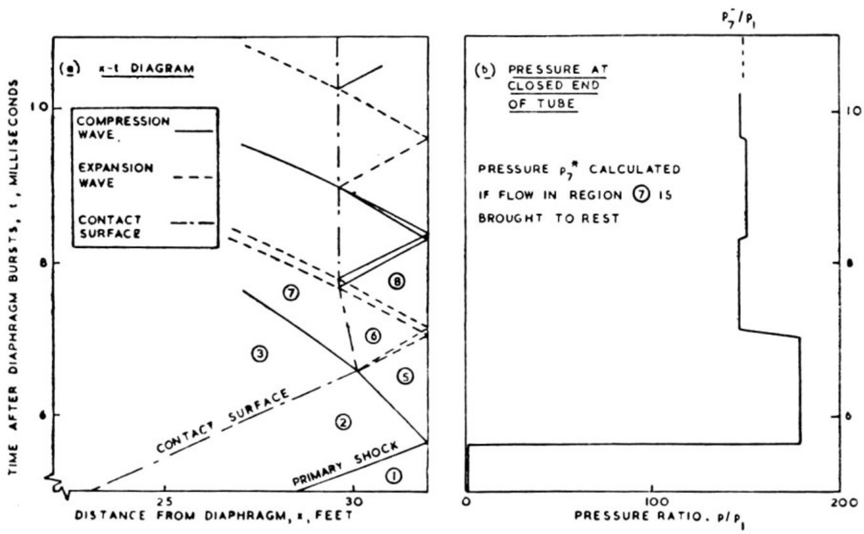

FIG. 6. Calculated wave diagram and pressure variations for a tube closed at $x = 32$, H_2/air, $M_{s1} = 5{\cdot}09$.

This difficulty may be overcome[10] by heating the driver gas in order to change the Mach number for tailoring. An alternative approach has, however, been studied at the N.P.L. in order to avoid possible difficulties in uniformly heating high-pressure hydrogen. Here the strengths of successive disturbances in the reflection process the end between of the tube and the contact surface have been studied[9], in the hope that they will rapidly become weak. A typical calculated wave pattern is presented in Fig. 6, together with the associated pressure changes at the nozzle entry. It is seen that, after the first reflected disturbance, successive disturbances are relatively weak; the contact surface is brought effectively to rest, and the pressure rapidly approximates to the value p_7^* calculated on the assumption that the flow behind the first transmitted shock is brought isentropically to rest. Calculations for other shock Mach numbers lead to similar conclusions.

These results suggest that if the time after the first reflected disturbance is used for test purposes, long running times may be achieved by reflected-shock operation even under conditions far removed from "tailoring".

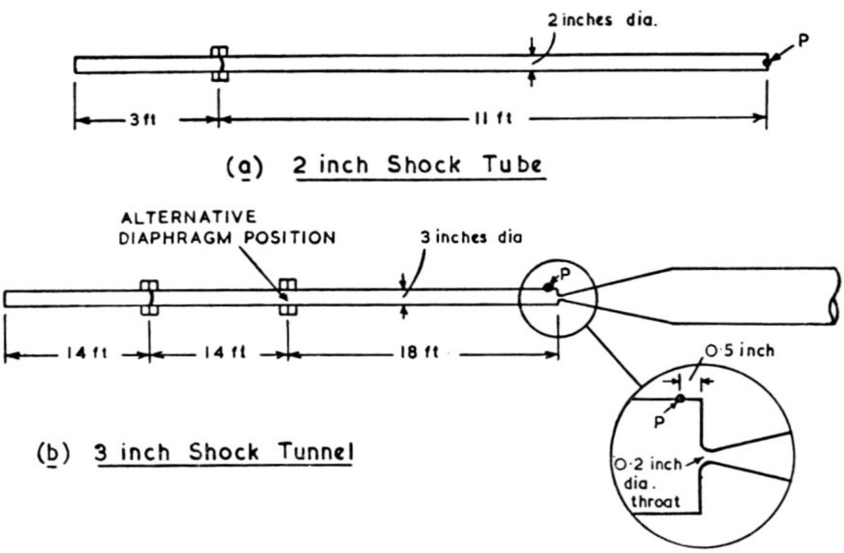

FIG. 7. Details of the shock tube and shock tunnel used for the experimental work. (P denotes pressure transducer).

Thus, referring to Fig. 3, the duration of uniform conditions at the nozzle entry is t_0 for "straight-through" operation, t_1 if the uniform flow is terminated by the first disturbance reflected from the contact surface, t_2 if subsequent disturbances are negligible, and t_3 if "tailored" conditions are achieved. The rate of movement of the contact surface towards the nozzle entry is determined on considerations of the continuity of mass by the rate of flow into the nozzle throat, an approximate relationship between t_3 (or t_2) and t_0 being (H_2/Air) $t_3/t_0 \approx 0{\cdot}8\ A_D/A_T$, where the ratio of the cross-sectional area, A_D, of the driving tube to that, A_T, of the throat is typically of order 100. The time before the arrival of the first reflected disturbance is not wasted, since it may be used in the establishment of the flow in the nozzle, and past the model under test.

3.2.2. *Comparisons with experiment*—To provide data for comparison with the simple theoretical results outlined above, pressure measurements have been made[9] in the small shock tube and shock tunnel sketched in Fig. 7. Typical pressure traces measured to the end of the shock tube,

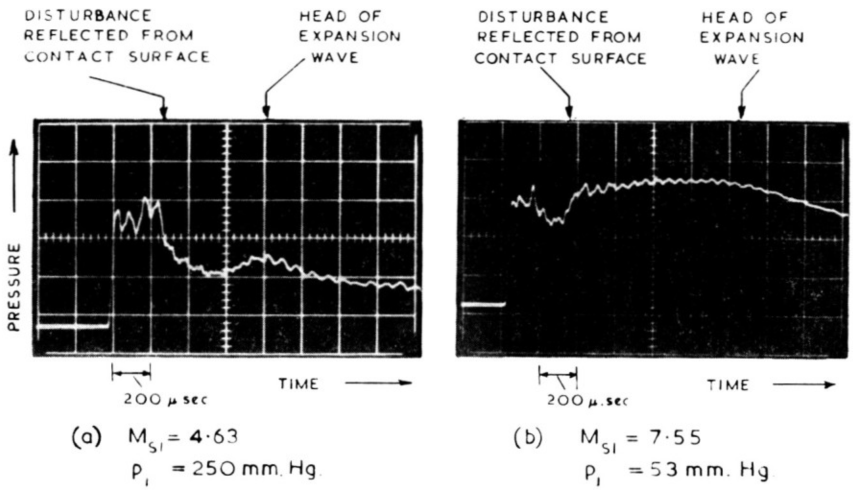

FIG. 8. Typical pressure records at the closed end of the 2 in. dia. shock tube (Fig. 7a). H_2/air.

and near the nozzle entry of the shock tunnel, are reproduced in Figs. 8 and 12. The pressure rise immediately after the reflection of the shock is in good agreement with real-gas theory, but there is then a marked fall of pressure. This occurs before the arrival of the disturbance reflected from the contact surface, and is attributed mainly to attenuation of the reflected shock[12] due to its interaction with the boundary layer formed on the wall of the tube. This pressure fall has been observed* in all measurements made at the N.P.L. in the 2 in. and 3 in. diameter tubes, but is not so pronounced in the 6 in. by 3½ in. tube used in the measurements illustrated in Fig. 5. It has not proved possible to explain this discrepancy on the basis of differences of Reynolds number, and further research is in hand to investigate the effects of the size and shape of the cross-section of the tube.

The position of the contact surface is, of course, greatly affected by viscosity, and in the N.P.L. experiments it has been detected by a probe

* The pressure fall is observed only at points very close to the end of the tube.

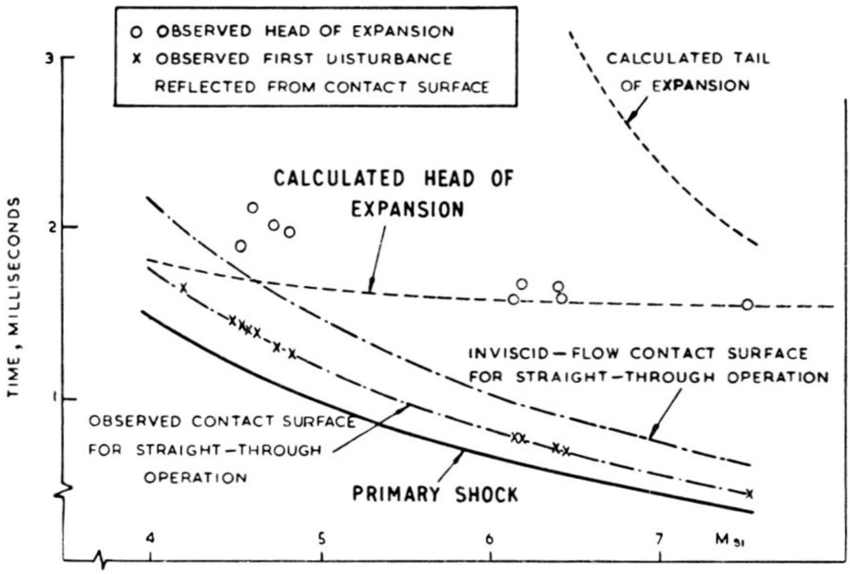

FIG. 9. Times of arrival of the major flow features at the end of the 2 in. dia. shock tube (Fig. 7a). H_2/air.

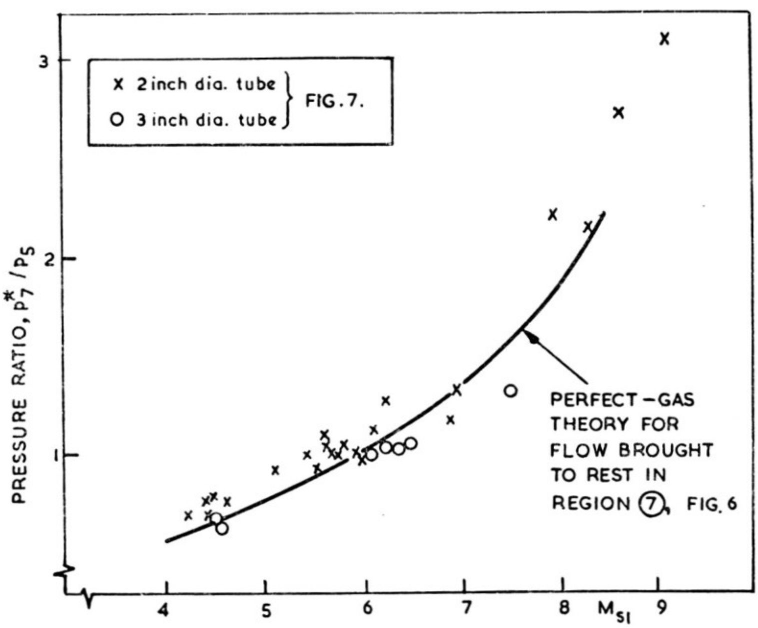

FIG. 10. Observed and calculated values of the quasi-uniform pressure after the initial disturbances reflected from the contact surface H_2/air.

fitted with a resistance thermometer. Typical results are reproduced* in Fig. 9. The time of arrival of the first disturbance reflected from the contact surface is, as predicted by simple theory, seen to be in good agreement with the time of arrival of the undisturbed contact surface. Calculations suggest that the strength of the disturbance reflected from the contact surface should not be greatly affected by attenuation of the reflected shock, and the measured strengths are seen in Fig. 4 to be in fair agreement with calculation. After the first disturbance, the pressure is seen in Figs. 8 and 12 to settle down to a reasonably uniform value, as predicted by calculation. This pressure level is shown in Fig. 10 to be in fair agreement with the calculated pressure p_7*, which assumes that the flow is brought to rest behind the first transmitted shock.

3.2.3. *Effects of the expansion wave originating at the diaphragm*—In a shock tube of fixed proportions, the reflected head of the expansion

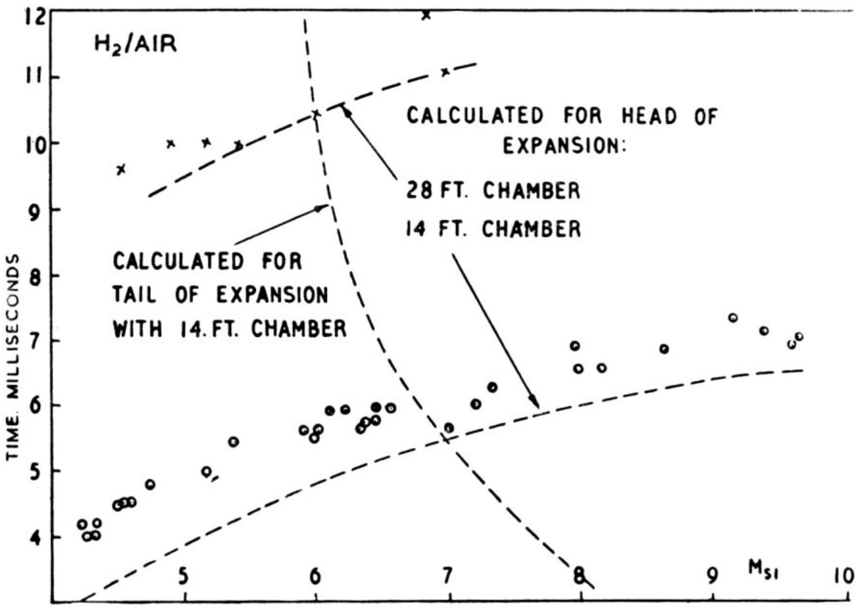

FIG. 11. Time of arrival after shock of expansion wave from primary diaphragm at end of 3 in. dia.

wave will usually arrive at the end of the tube before the tail at low shock Mach numbers, whereas the tail will arrive first at high shock Mach

* The curves for the arrival of the contact surface are referred to in Fig. 9 as for "straight-through" operation, since the times shown are those at which the contact surface would reach the end of the tunnel if its motion was not affected by the reflected shock. The curves have been derived from a slight extrapolation of data obtained at a distance from the end of the tubes sufficient for this condition to be satisfied.

numbers. This is illustrated in Fig. 11 where measured* and calculated values for the 3 in. shock tunnel are reproduced. The N.P.L. shock tunnels are fitted with alternative diaphragm positions, so that the length of the high-pressure chamber can be altered. Results for two chamber lengths are included in Fig. 11, and the effect on the uniformity of pressure at entry to the nozzle is illustrated in Fig. 12, where the duration of uniform pressure is increased from about 1 to about 7 msec by doubling the chamber length.

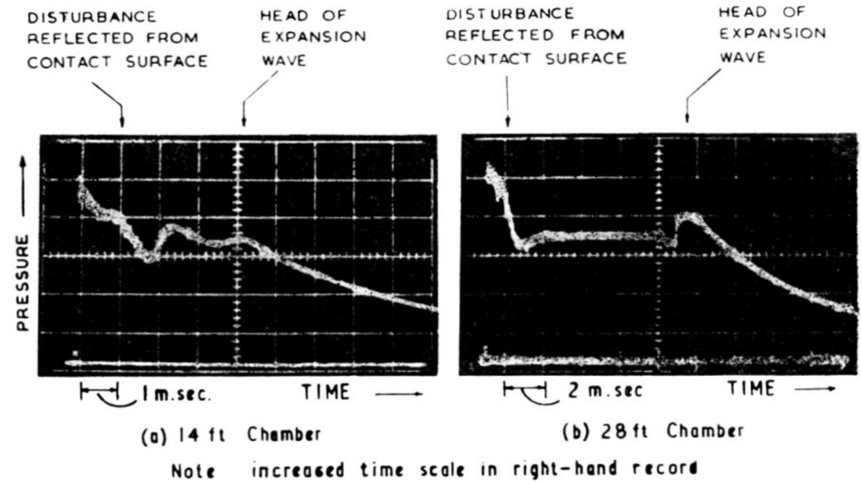

FIG. 12. Effect of increasing the length of the high-pressure chamber on the pressure near the nozzle entry of the 3 in. dia. tube (Fig. 7b). $M_{s1} = 4{\cdot}1$, H_2/air.

For reflected-shock operation, the arrival of the expansion wave usually imposes a more severe limitation to the duration of uniform conditions at the nozzle entry than does the arrival of the contact surface. As suggested by Wittliff(10), the limitation imposed by the arrival of the tail can, in theory, be removed by inserting a nozzle downstream of the primary diaphragm; it is also possible that the reflection of the head of the expansion wave can be cancelled by suitable design of the end wall of the high-pressure chamber. Research on these possibilities is in progress at the N.P.L.

4. THE ESTABLISHMENT OF STEADY FLOW PAST THE MODEL UNDER TEST

The useful testing time is also affected by the time required for the flow past the model to become steady. For the flow near the stagnation point of a bluff body, this time appears to be short, but for boundary

* No measurements are included for the tail of the expansion wave, because the pressure gradient there is too weak to permit its accurate detection.

layers and separated flows, longer periods may be required. Flows of these types have, therefore, been examined optically in a shock tunnel at the N.P.L.; they have included boundary layers on flat plates, separated flows up and down steps, and the flow past representative practical con-

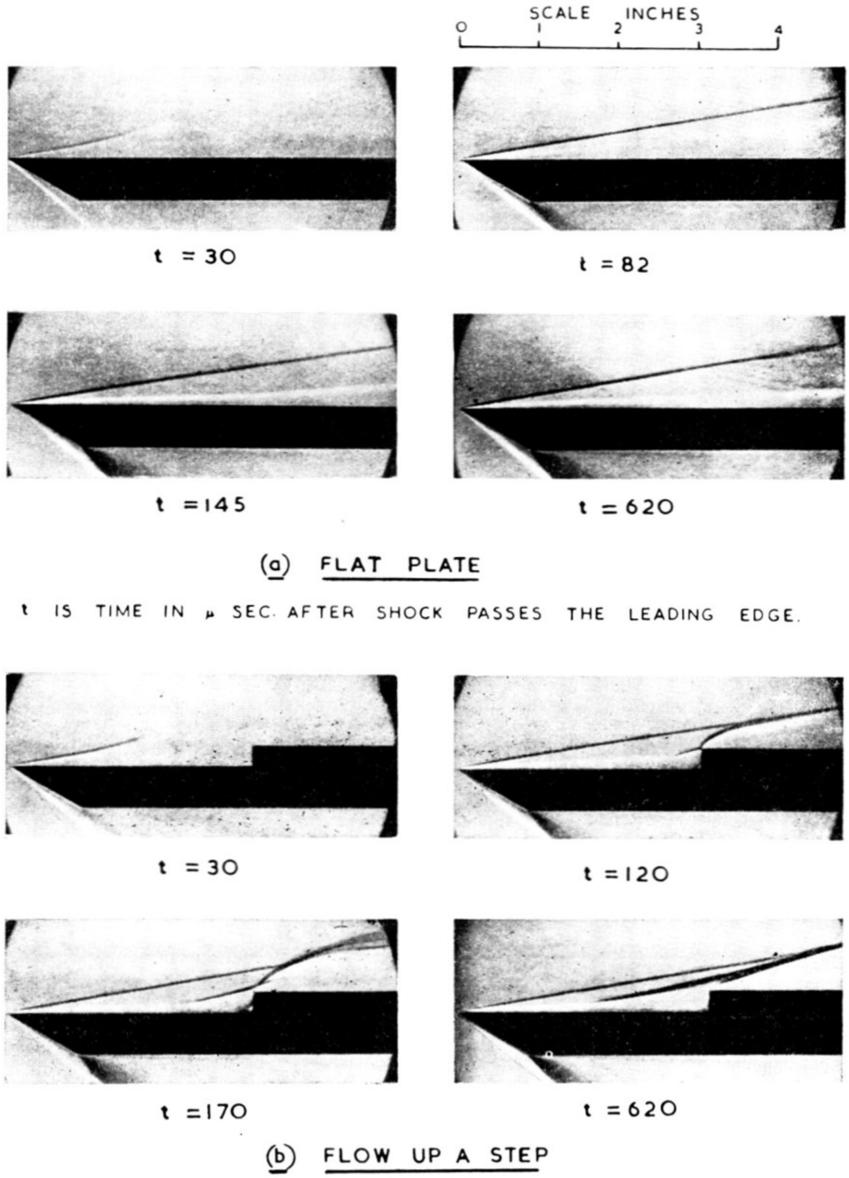

FIG. 13. Photographs illustrating the establishment of steady flow in a shock tunnel with $M_w = 6{\cdot}5$, $M_{s1} = 4{\cdot}0$, $p_1 = 650$ mm Hg. (See Fig. 12b for duration of flow at nozzle entry).

figurations. Examples of the results for a flat plate are shown in Fig. 13a, where it is seen that steady conditions are approached at about 600 μsec after the shock first strikes the model. The way in which the boundary layer develops is in striking contrast to what would be expected if the starting flow consisted of a plane shock followed by uniform conditions. It seems probable that the discrepancy is associated with the large increase of Reynolds number that occurs after the initial passage of the shock past the model, due to the strong expansion wave that follows the shock for large pressure ratios across the nozzle diaphragm. A different explanation must, however, be used to explain the development of the separated flow up a step illustrated in Fig. 13b, where the shock associated with the separation point is seen to move forward to its steady flow position. It seems likely that the speed of upstream propagation of the shock reflected from the step may play an important part. Measurements of the heat transfer to the flat plate suggest that the heat-transfer rate takes considerably longer (e.g. 2 msec) to become steady than does the flow pattern visualized by Schlieren methods.

As far as the present paper is concerned, the most important conclusion that may be drawn from preliminary investigations of this type is that the time taken to achieve steady conditions may be appreciable, but is well within the available running time, at least if the shock Mach number is not too large.

5. MEASURING TECHNIQUES

Investigations of the type outlined above suggest that reasonably long running times can be achieved in reflected-shock tunnels over a useful range of shock Mach number. Considerable effort is, however, required in the development of measuring techniques, not only to achieve sufficiently rapid response times, but also to measure quantities which are of no interest in usual wind-tunnel practice, but become important in the presence of high-temperature real-gas effects. Certain N.P.L. investigations on the development of techniques are outlined briefly below.

5.1. *Force Measurements*

The relatively long flow durations in large shock tunnels enable conventional strain-gauge balances to be used at the lower test section Mach number (e.g. $M_w \leqslant 6$) where the forces on models, typically, exceed 10 lb. For example, a standard 6 component wind-tunnel balance designed for normal forces of 50 lb was found to have a natural frequency of 1·2 kc/s when modified by removing as much spring weight as possible. With sufficient amplification before the recording equipment, it is desirable to use stiff, and hence insensitive, strained members in order to obtain a high natural frequency. At high test-section Mach number, however, the forces become very small, and cannot be measured with sufficient accuracy with a strain gauge balance of adequate frequency response.

An accelerometer technique is being developed for use under these conditions, and for this purpose electroformed copper models with skins 0·005 in. thick and weighing about 0·02 lb have been made. Adding to this the weight (0·02 lb) of an accelerometer having a sentisivity of 10 m/Vg the overall sensitivity of the system is approximately 250 mV/lb of aerodynamic force. It should, therefore, be possible to measure forces of about 0·1 lb. Drag measurements only are at present being made, and for this purpose the model is suspended initially by fine threads; it is caught on a spigot after moving a distance slightly longer than that travelled in the flow duration.

5.2. *Pressure Measurements*

The range of pressures to be measured in shock tunnels is large, extending from the pressure behind the reflected shock, which may be 1000 atmospheres, to the static pressure in the test section which may be as low

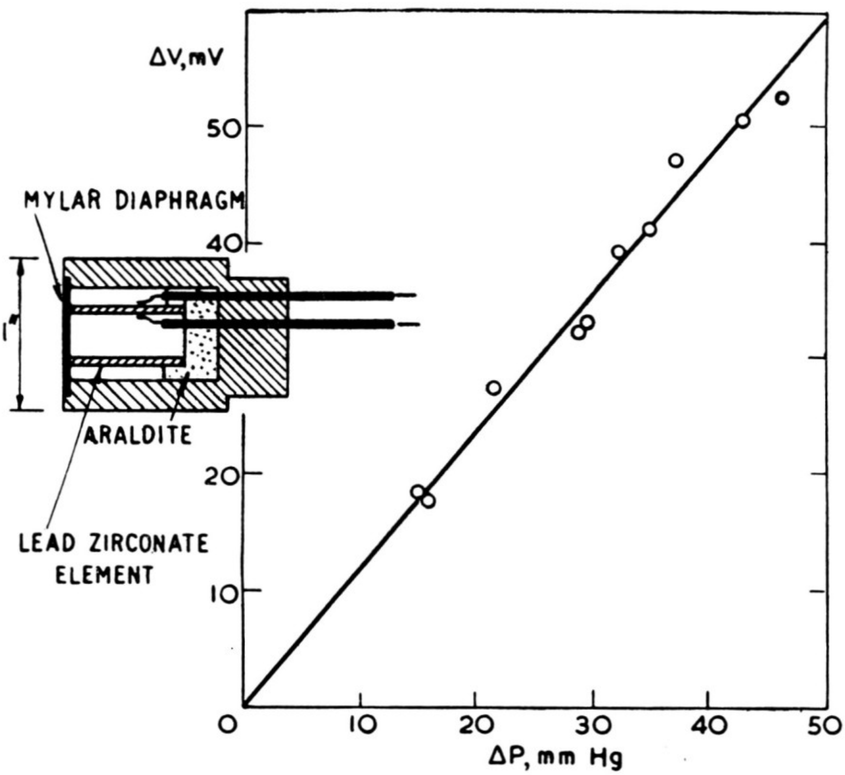

FIG. 14. Calibration of N.P.L. pressure transducer.

as 1 mm of mercury. The higher pressures present no difficulties, and commercial quartz transduceres have been used at the N.P.L., because of their inherent linearity and stability. Resilient mountings made from equal proportions of Araldite 103 and Thiokol Chemical Corp. Liquid Polymer LP3 have been used successfully to reduce vibration effects.

A sensitive pressure transducer developed at the N.P.L. for use in the test section is shown in Fig. 14, together with its calibration curve. The hollow cylindrical piezo-electric element is mounted in Araldite, and the load is transmitted by means of a Mylar diaphragm 0·007 in. thick; the natural frequency of the complete transducer is 30 kc/s. The sensitivity is 1·19 mV/mm Hg, which is adequate for most applications, provided that the acceleration of the model is kept low by the use of rigid supports isolated from the shock-tunnel structure.

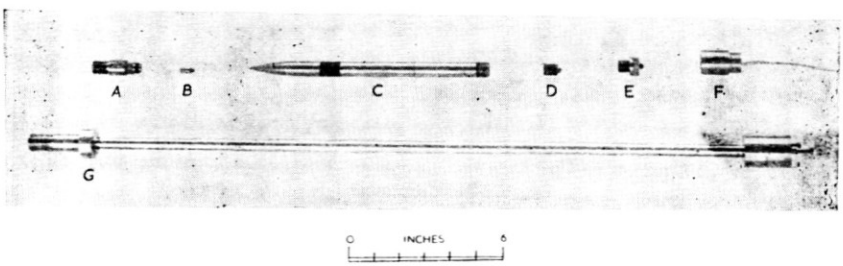

	A	B	C	D	E	F	G
MAKER AND TYPE	SLM PZ 14	SLM PZ6	ARC BC 33	ARC BC 60	ARC BC 65	NPL*	NPL
SENS. pCb/mm Hg	0·68	0·001	12·0	3·2	4·3	3·6	2·3
F_{nat} K c/s	49	250	80	66	60	33	TIMES LESS THAN 660 μ SEC

* FIG. 14

FIG. 15. Pressure transducers for use in shock tunnels.

Fig. 15 includes a photograph of a range of pressure transducers used in the N.P.L. shock tunnels, together with details of their manufacturers*, sensitivities and natural frequencies†.

* SLM denotes the Swiss Locomotive Company, Winterthur, Switzerland, and ARC the Atlantic Research Corporation, Alexandria, Virginia, USA.

† For the bar gauge, the time quoted is that when the stress wave reflected from the end of the bar strikes the piezo-electric element.

5.3. *Flow Visualization*

Extensive use has been made of Schlieren photography on the N.P.L. shock tunnels using single or multiple-spark light sources, wave-speed cameras, or high speed cine cameras. The equipment used for most of this work involves no new developments, and a few points only will be mentioned here.

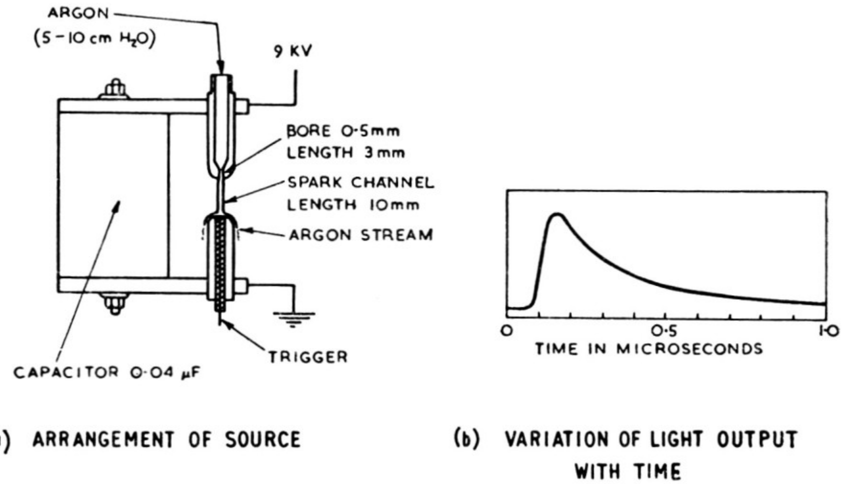

FIG. 16. A spark light source with an open cap and stabilization of the spark channel by means of an argon jet.

After experience with a wide range of spark light sources(13), an open gap in which the position of the discharge is located(14, 15) by a fine laminar jet of argon issuing from one electrode (see Fig. 16) is now used on all facilities. This is found to give very reliable results, coupled with the short exposure time (about 0·2 μsec above half amplitude) required for shock-tube work. An assembly of five such gaps arranged to provide a multiple-spark source* for Cranz-Schardin photography is shown in Fig. 17.

For wave-speed camera photography using a continuous light source and drum camera, it is necessary to provide a shutter which opens for one revolution of the drum, and is triggered by a signal produced, for example, by the passage of the shock past a detector in the shock tube. In such cases, the delay that can be accepted between the arrival of the signal and the opening of the shutter is often small (e.g. 100 μsec), and for high film speeds a shutter is required which, when open, transmits most of the incident light. A spark-operated mechanical shutter has been developed at the N.P.L. for this purpose, and is illustrated in Fig. 18, together

* An earlier multiple-spark source employing eight end-fire gaps is described in ref. 15.

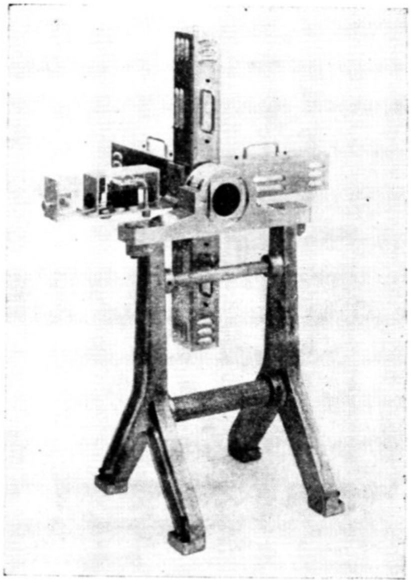

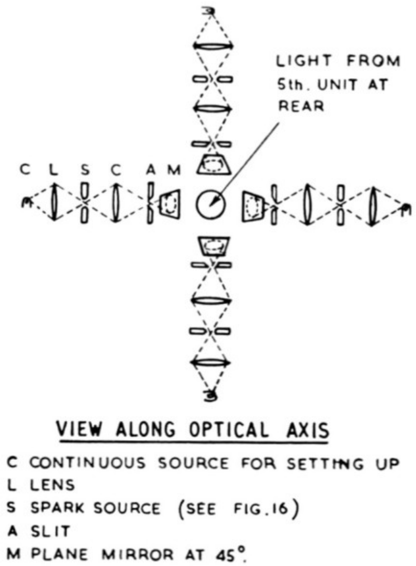

FIG. 17. A 5-channel multiple-spark source for Crauz-Schardin photography.

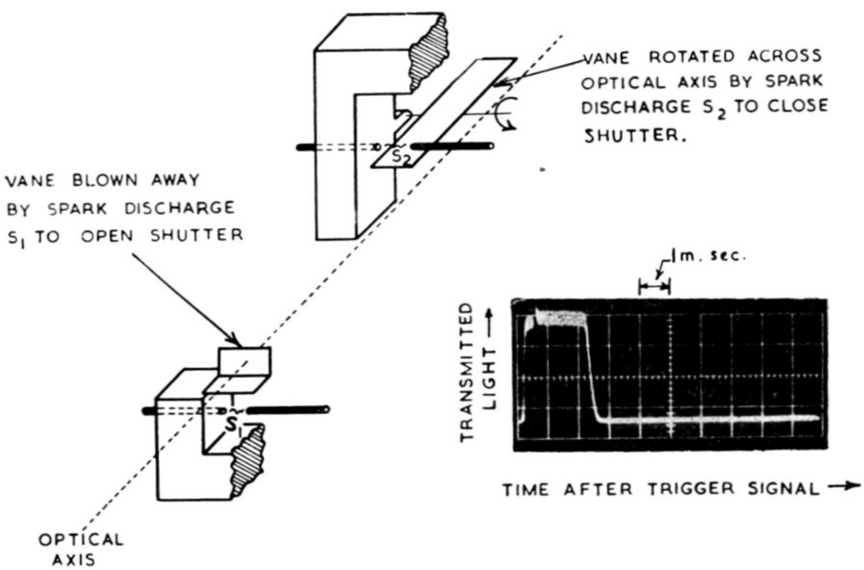

FIG. 18. A spark-operated shutter for drum-camera photography with a continuous light source.

with the wave-form of the transmitted light as measured with a photo-multiplier. For reasons of clarity, the delay between the operation of the sparks has been adjusted so that the parts of the trace corresponding to the opening and closing of the shutter are separated by a long time interval (2 msec).

5.4. *Heat-Transfer Measurements*

The well-established thin-film resistance-thermometer method has been used[16, 17] at the N.P.L. in several investigations of heat transfer at rates up to 40 kW/in^2, although the scatter of the derived data (which may be as much as ± 15 per cent) is still considered unsatisfactory. The platinum thermometer films are painted and baked on the surface, and are calibrated by discharging a condenser through them at constant current.

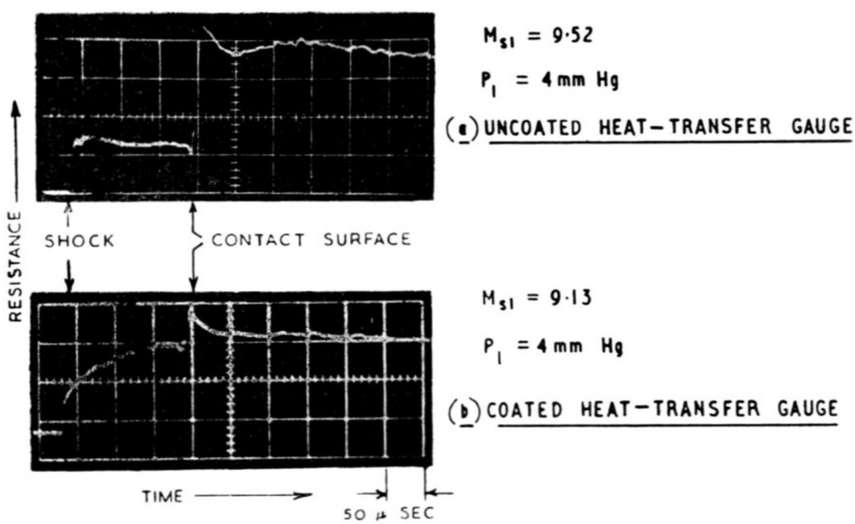

FIG. 19. Effect of SiO_2 coating on the output of a resistance thermometer in the presence of ionized gas.

The errors may arise from several sources. It is possible that the thickness of a film is not uniform*, and that an error is thereby introduced because, in calibration, the local heating rate is a function of thickness. Edge effects in calibration may also produce errors[19], and further errors are introduced in reading oscillograph traces. In the heat-transfer rate is not constant during an experiment, an additional error may arise, because the instantaneous rate depends on the previous temperature history of

* Sputtered films have a more uniform thickness[18], but it is more difficult to apply them to curved surfaces.

the film. Research is in progress to reduce these errors, and to develop an analogue technique to simplify the reduction of the data.

For use in ionized gases, the thermometer elements are coated with SiO_2 to provide electrical insulation, and the signal obtained from uncoated and coated films located at the stagnation point of a bluff body are compared in Fig. 19. Experiments, made in the absence of ionization, show that the presence of the coating has no measurable effect on the heat-transfer rate.

5.5. *Ionization Measurements*

Studies of the ionization of shock-heated gases are important in connexion with the propagation of radio signals, and in determining whether de-ionization occurs when the gas is cooled on expansion in the nozzles of hypersonic test facilities working at high enthalpy. Microwave techniques have been used at the N.P.L. for shock-tube studies of ionization in argon[(20)], and in air[(21)]; a sketch of the apparatus, and typical results for air, are reproduced in Fig. 20.

For a given initial pressure, p_1, of the test gas, the predominant effect at low shock Mach numbers, M_{s1}, is that of the elastic collision of electrons with neutral molecules and atoms; the gas behaves as a lossy dielectric with small absorption, as shown in the lower inset trace. Under these conditions, a measurement of the absorption may be used to derive the product of the electron density and collision frequency. At higher shock Mach numbers, the electron density approaches or exceeds the critical value where the gas is totally reflecting and no energy is transmitted; a typical trace is reproduced in the upper inset of Fig. 20. The point at which all incident power is reflected is independent of collision frequency*, so that one value of the electron density may be derived unambiguously for each value of the radio frequency. For example, with $M_{s1} = 11{\cdot}5$ and $p_1 = 1$ mm of mercury, the electron density determined in this way is $6{\cdot}6 \times 10^{11}$ per cm^3 which agrees well with calculation.

It is reasonable, therefore, to assume that the theoretical values of the electron density are correct at other shock Mach numbers, where the absorption depends also on the collision frequency. The agreement between the calculated and measured values illustrated in Fig. 20 then suggests that the predicted values of the collision frequency are also correct. An approach of this type is necessary, because only a limited number of radio frequencies is available for the microwave system, and because the frequencies do not extend to values large enough to penetrate the high electron densities occurring, for example, at the entry to the nozzle of a shock tunnel.

---

* Provided that the collision frequency is small compared with the radio frequency.

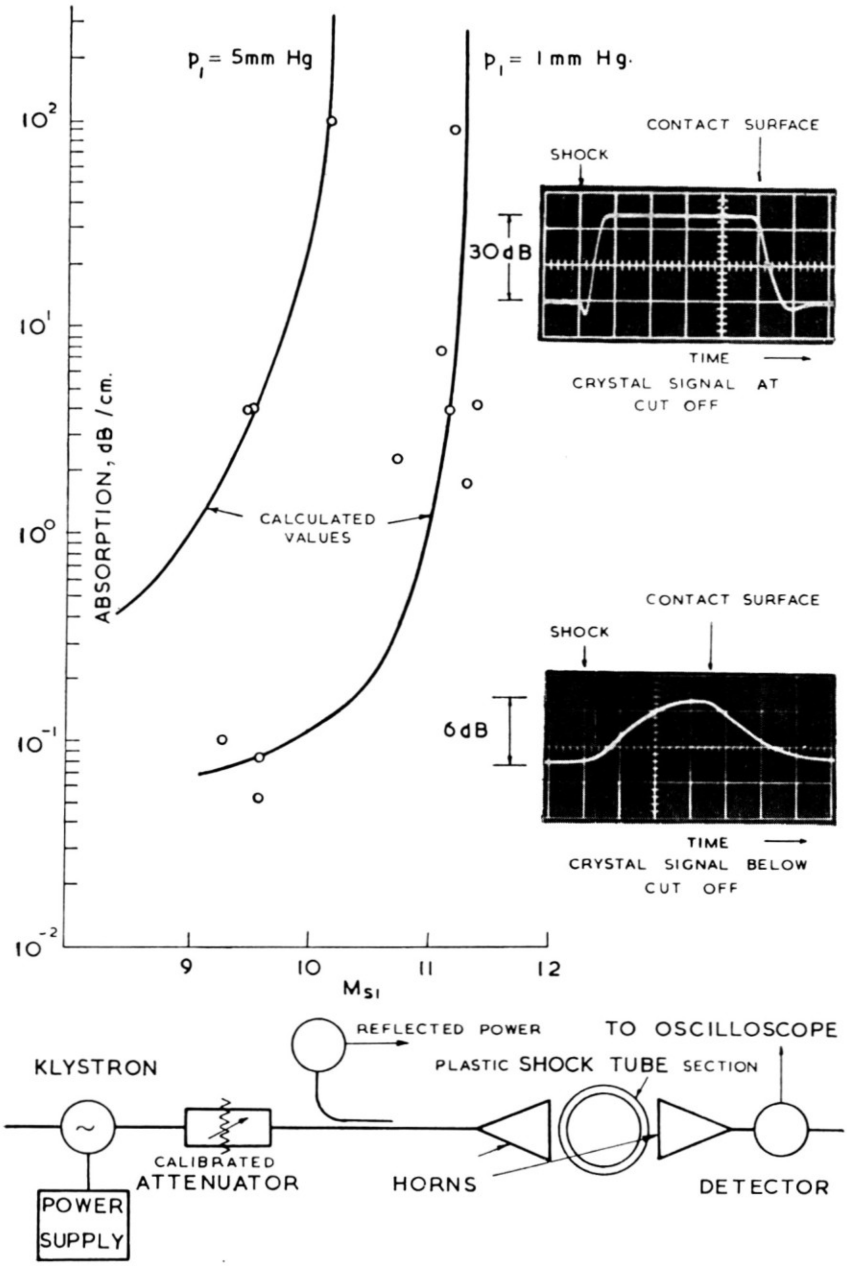

FIG. 20. Absorption of microwaves in ionized air, frequency $= 7{\cdot}29 \times 10^9$ c/s.

It should be noted that the collision frequency is an integrated effect of all atomic and molecular species, and that a single measurement of the type described is not sufficient to determine whether all of these species are present in their equilibrium concentrations. For air at temperatures below 5000°K, the most important contributions to the collision frequency are due to n_2, o, and no, and it seems unlikely that any large errors in the predicted concentrations would have passed undetected.

5.6. *Spectrographic Techniques for Temperature Measurement*

It has been shown that the pressure at entry to a shock-tunnel nozzle may remain substantially constant for several milliseconds, but it is also important to determine the variation of stagnation temperature. For temperatures up to about 3000°K, the sodium-line reversal method[22] can be used, and recent research[23] at the N.P.L. has concentrated on the measurement of higher temperatures. One method that has been studied, is to observe the relative intensities of emission and absorption lines produced by impurities in the gas. A line absorption spectrum obtained by observing a flash tube of high brightness temperature through the shock-heated gas enables the equivalent widths of the impurity lines to be obtained, and these, together with the emission spectrum, enable the temperature of the gas to be deduced without knowing the temperature of the flash tube.

Acknowledgement—The paper is presented by permission of the Director of the National Physical Laboratory.

REFERENCES

1. Lukasiewicz, J., Experimental Investigation of Hypervelocity Flight. Proc. 1st International Congress of the Aeronautical Sciences, Madrid, 1958
2. Henshall, B. D., The Use of Multiple Diaphragms in Shock Tubes. British Aeronautical Research Council, Current Paper 291, 1956
3. Bray, K. N. C., Departure from Dissociation Equilibrium in a Hypersonic Nozzle. British Aeronautical Research Council, Report 19, 983, 1958
4. Freeman, N. C., Non-Equilibrium Theory of An Ideal Dissociating Gas in a Conical Nozzle. British Aeronautical Research Council, Report 20, 430, 1958
5. Nagamatsu, H. T., Workman, J. B. and Sheer, R. E., Hypersonic Nozzle Expansion with Air Atom Recombination Present. General Electric Research Laboratory Report No. 60–RL–2332C, 1960
6. Henshall, B. D., Experimental Results from the N.P.L. Hypersonic Shock Tunnel. *Hypersonic Flow*, p.1, Butterworths, 1960
7. Henshall, B. D. and Gadd, G. E., Factors Affecting the Performance of the Nozzle of a Hypersonic Shock Tunnel. British Aeronautical Research Council, Current Paper 293, 1956
8. Holder, D. W., Experimental Facilities and Measuring Techniques for Research on Hypersonic Flow. *J. Aeronaut. Sci.* **63**, 493, 1959

9. HOLDER, D. W. and SCHULTZ, D. L., On the Flow in the Reflected-shock Tunnels. British Aeronautical Research Council, Report 22, 152, 1960
10. WITTLIFF, C. E., WILSON, M. R. and HERTZBERG, E., The Tailored-Interface Hypersonic Shock Tunnel. *J. Aeronaut. Sci.* **26**, 219, 1959
11. HOLDER, D. W., STUART, C. M. and NORTH, R. J., Shock-tube Studies of the Interaction of a Reflected Shock with the Bondary Layer and Contact Surface. British Aeronautical Research Council, Report (In preparation)
12. MARK, H., The Interaction of a Reflected Shock Wave with the Boundary Layer in a Shock Tube. Cornell University Report AFOSR-TN-57-345, AD 132-418, 1957
13. HOLDER, D. W. and NORTH, R. J., Optical Methods for Examining the Flow in High-Speed Wind Tunnels. *AGARDograph* 23, *Part* 1, 1956
14. THACKERAY, D. P. C., Preferential Ionization of Argon in the Presence of Air and its Application of Electric Discharge Devices. *Nature* **180**, 913, 1957
15. NORTH, R. J., A Cranz-Schardin High-Speed Camera for use with a Hypersonic Shock Tube. *Proceedings of the 4th International Congress on High-Speed Photography*, Cologne, 1958
16. HENSHALL, B. D. and SCHULTZ, D. L., Some Notes on the Use of Resistance Thermometers for the Measurement of Heat-Transfer Rates in Shock Tubes. British Aeronautical Research Council, Current Paper 408, 1959
17. HENSHALL, B. D., Stagnation-point Heat-Transfer Rate Measurements in the Unexpanded Flow of the N.P.L. Hypersonic Shock Tunnel. British Aeronautical Research Council, Report 20, 716, 1959
18. RABINOWICZ, J., JESSEY, M. E. and BARTSCH, C. A., Resistance Thermometers for Heat-Transfer Measurements in a Shock Tube. California Institute of Technology, Hypersonic Research Project Memo. No. 33 1956
19. SPENCE, D. A., Two Heat-Diffusion Problems with Shock Tube Applications. British Aeronatical Research Council, Report 21, 536, 1959
20. SCHULTZ, D. L., Shock-Tube Research at the N.P.L. on the Properties of Gases at High Temperatures. Part 1. Ionization Measurements. *Hypersonic Flow*, p.301, Butterworths, 1960
21. SCHULTZ, D. L., Microwave Studies of the Properties of Ionized Air in a Shock Tube. *Proc. of the 4th International Conference on Ionization Phenomena in Gases*, Uppsala, 1959
22. CLOUSTON, J. G., Temperature Measurements of Shock Waves by the Spectrum-line Reversal Methods. *Proc. Roy. Soc. A*, **248**, p.429, 1958
23. LAPWORTH, K. C., Shock-Tube Research at the N.P.L. on the Properties of Gases at High Temperatures. Part 2. Preliminary Spectrographic Measurements. *Hypersonic Flow*, p.317, Butterworths, 1960

DISCUSSION

J. VALENS: Ainsi que Monsieur le Professeur G. Bock, Président de Séance, a bien voulu l'annoncer, je voudrais présenter avec l'accord de M. le Professeur Maurice Roy, Président du Programme du Congrès, quelques résultats d'expériences obtenus à Marseille à l'Institut de Mécanique des Fluides. Il ne s'agit pas en fait d'une communication préparée à l'avance mais d'une simple intervention constituant en quelque sorte une illustration sur un exemple particulier, de ce que l'on peut attendre des techniques d'essais qui viennent de faire l'objet du brillant exposé du Dr. D.W. Holder. Mais auparavant je voudrais rendre hommage au travail accompli au National Physical Laboratory par l'excellente équipe que cet Auteur a su réunir autour de lui.

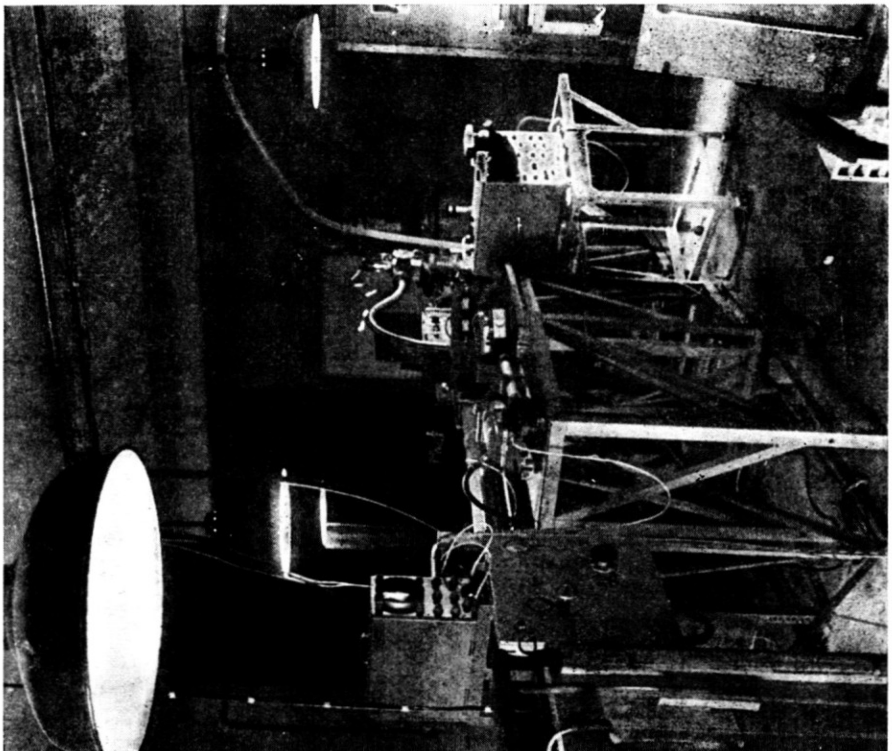

Fig. 1

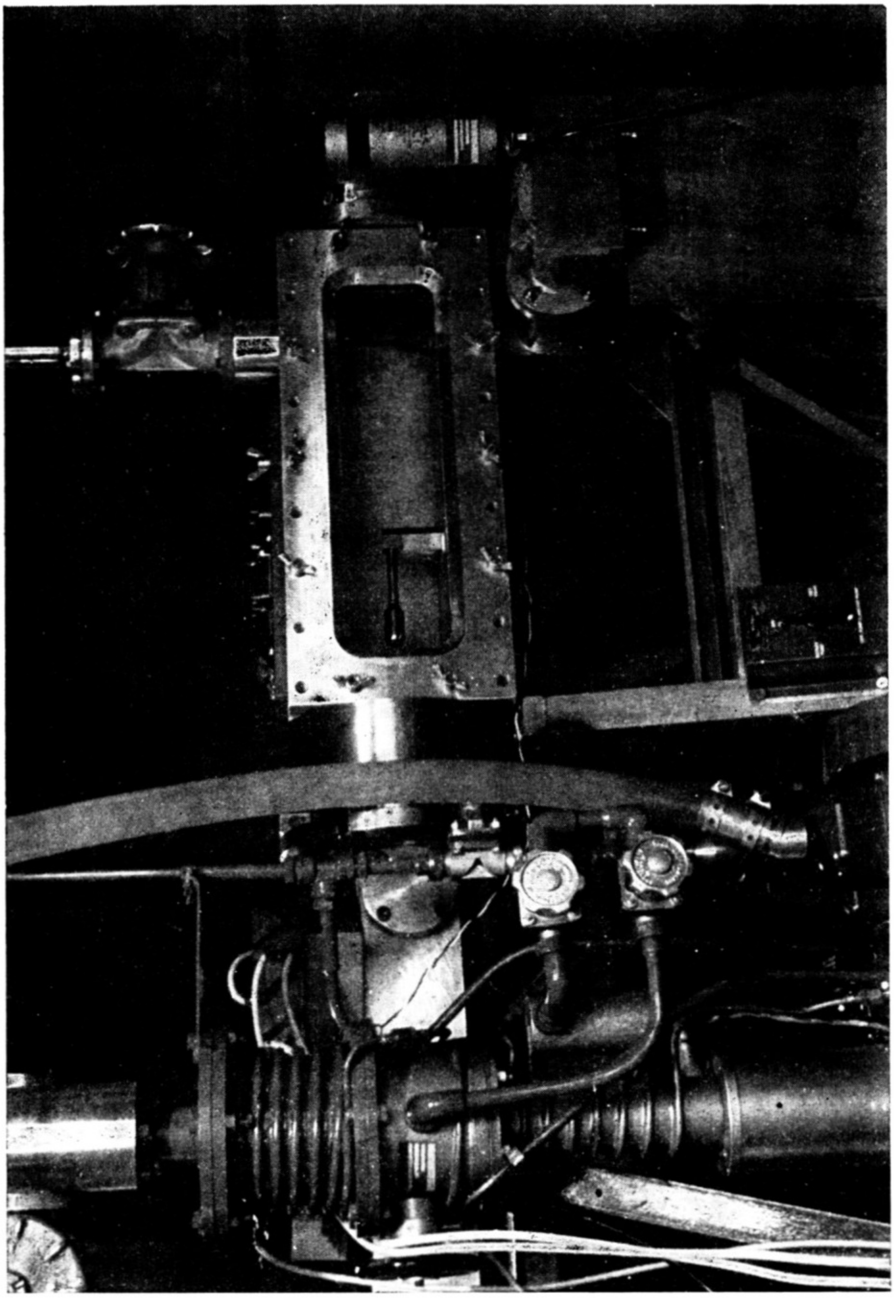

FIG. 2.

Aussi bien les techniques utilisées à Marseille sont, avec quelques variantes, semblables à celles mises en oeuvre au National Physical Laboratory, elles-mêmes inspirées des travaux de Cornell University et d'AVCO.

La figure 1 est une vue du tube à choc que nous utilisons. Il possède une chambre de l'haute pression que l'on remplit d'hydrogène à 80 kg/cm² au maximum, et qui est suivie du tube d'essais de 4 m de longueur environ et de section carrée, de 4 cm de côté.

On peut adjoindre à ce tube une chambre de détente, visible dans la figure 2, et qui comporte une tuyère conique, permettant de réaliser par la technique du choc réfléchi décrite par le Dr. Holder, et dans les meilleures conditions d'adaptation, des rafales d'une durée de 150 μsec environ à $M = 6{\cdot}7$, avec une température d'arrêt de l'ordre de 4000°K.

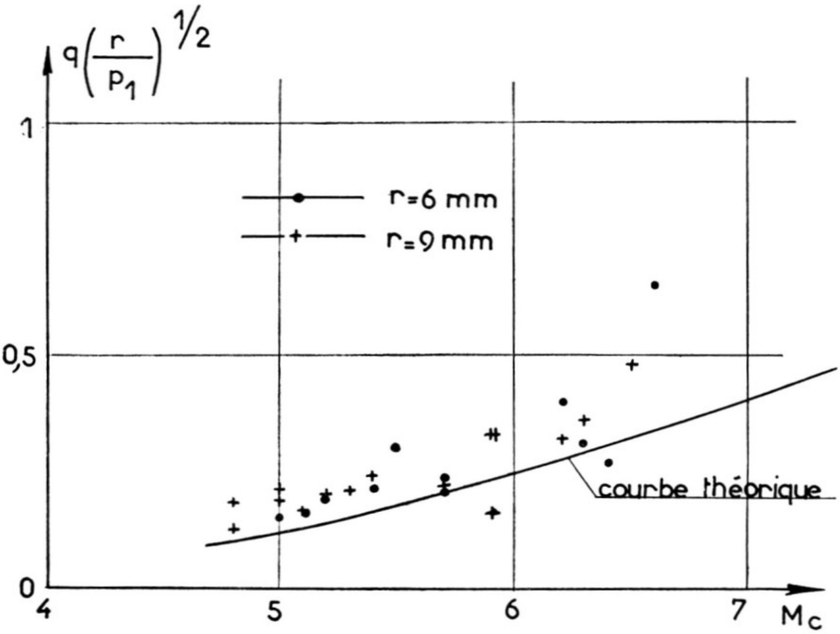

FIG. 3.

Il s'agit en fait d'une installation pilote que nous utilisons pour la mise au point des techniques d'essais et qui nous a permis d'établir le projet d'un tube plus important, actuellement en cours de montage, qui comporte un tube d'essais de 9 m de long et où pourront étre réalisées des rafales d'une durée de 800 μsec, environ à $M = 12$, avec une température d'arrêt de 8000°K environ.

La figure 3 extraite d'un rapport intérieur[1] rassemble les résultats des mesures de taux de transfert de chaleur au point d'arrêt d'un corps hémisphère cylindre, que nous avons exécutées dans le tube à chocs pilote, à l'aide de maquettes en Pyrex placées à l'extrémité du tube d'essais à section constante. La technique utilisée est celle du thermomètre à film de platine. On a porté en ordonnées le flux de chaleur réduit, $q\left(\frac{r}{p_1}\right)^{1/2}$,

---

[1] P. Micheau et H. Guenoche, "Mesures de transfert de chaleur au point d'arrêt pour des sphères de différents rayons, "Rapport I.M.F.M., Juillet 1960 (Essais effectués à la demande du Service Technique de l'Aéronautique, Bureau "Etudes Générales").

où q représente le flux de chaleur unitaire exprimé en kw/cm²/sec, où r représente le rayon de la sphère exprimé en mm et p_1 mm de hg, la pression initiale d'azote dans le tube d'essais. On a porté d'autre part en abscisses, le Mach du choc Mc, dont la variation était obtenue par la variation de p_1.

On a représenté sur la même figure, en trait plein, le taux de transfert réduit calculé d'après l'expression donnée par Fay et Ridell.

Les grandeurs intervenant dans cette expression ont été calculées d'après les équations du choc droit, en tenant compte des effects des gaz réels et en utilisant les valeurs mesurées du Mach de choc M_c et de la pression p_1. Précisons d'ailleurs que le coefficient de viscosité absolue a été calculé à partir de l'expression fournie par la théorie cinétique des gaz, en utilisant pour les forces intermoléculaires, le potentiel de Lennard; le nombre de Prandtl a été pris égal à 0·71.

On voit que les points expérimentaux sont bien groupés autour d'une courbe dont l'allure est bien représentée par l'expression de Fay et Riddell. Toutefois les valeurs mesurées du flux réduit (gaz moteur: hydrogène; gaz d'essais: azote), sont légèrement supérieures aux valeurs théoriques. La loi de simplitude concernant le rayon de courbure au point d'arrêt est bien vérifiée.

D. W. HOLDER: It is gratifying to learn of the progress made by Professor Valens with the development of his shock tunnel. We were particularly interested by the result shown in Fig. 3 of his contribution, since our measurements in air of the heat transfer to the stagnation point of a sphere give results below rather than above the theory of Fay and Riddell.

T. SPRINKS: I was interested to see the photographs demonstrating the starting process over a flat plate in the N.P.L. shock tunnel (Fig. 13a). At Southampton a similar movement of the boundary layer has been witnessed in the starting process over bodies of revolution in the gun tunnel. The boundary layer growth in Fig. 13a immediately suggests either transition or laminar separation. The latter being probable in view of Dr. Holder's remark that the Reynolds' number increases after the initial passage of the shock past the model. Is it not then possible that the same process is occurring in Fig. 13b but this time with laminar separation downstream of the step? I should be very grateful if the authors would comment on this, and would like to know whether they have any other experimental information which indicates flow separation or otherwise.

D.W. HOLDER: We entirely agree that there may be laminar separation during the early stages of the starting process for the flow past the flat plate illustrated in Fig. 13a. Laminar separation may also occur downstream of the step shown in Fig. 13b, but we have no direct evidence of this. Results obtained for different step positions along the plate suggest, however, that the conditions upstream of the step are insensitive to those downstream.